# MORPHOLOGICAL STUDY OF THE MEANS OF ACCOMMODATION OF ADMIXTURE ATOMS IN THE CRYSTAL STRUCTURE OF MOLYBDENITE

Inna M. Kulikova, Inna E. Maximyuk
*Federal State Unitary Organization Institute of Mineralogy, Geochemistry, and Crystal Chemistry of Rare Elements, Moscow, Russia,*
*kulikova@imgre.ru, maximyuk@imgre.ru*

Accommodation modes of trace elements were studied in molybdenite from porphyry copper, quartz vein greisen and other ore types by means of microprobe analysis (on a Camebax-microbeam) and morphological analysis of secondary-electron images (SEI, on a Jeol 6700F scanning electron microscope). Molybdenite is one of the main minerals concentrating Re. Our microprobe analysis do not show any differences in the Re distribution in molybdenite from deposits of different genetic types. Re concentrations above the detection limit (0.04 – 0.05 wt.%) were found only at 98 analytical spots of the analyzed 284 spots. These proportions practically do not change at Re concentrations in the specimens varying within the range of 80 – 1100 ppm. Analysis of the secondary-electron images makes it possible to identify structural defects of crystals in the examined specimens: splitting into thin sheets (0.05 – 0.50 μm thick), intense growth of dendrites and the development of screw, edge and other types of dislocations (1 – 6 μm in characteristic size). Hexagonal pits (negative crystals) geometrically corresponding to crystals of the hexagonal 2*H* molybdenite polytype testify that our specimens are dominated by this polytype, with triangular pits geometrically corresponding to crystals of the 3*R* trigonal (rhombohedral) polytype found very rarely. The accommodation modes of minor elements in the molybdenite structure are controlled first of all by structural defects and Re atoms are often concentrated at dislocations.
7 figures, 15 references.
Keywords: molybdenite, polytype, rhenium, morphological analysis, dislocation.

## Introduction

Modern analytical techniques make it possible to study minerals at micro- and even nanometer scales. Molybdenite has been extensively studied by a diversity of physical (X-ray diffraction topography, electron microscopy, etc.) and chemical (calorimetric analysis, etching-pit method, etc.) techniques. This mineral is a principal concentrator of Re, an element of paramount importance for modern industry, whose individual minerals are very rare and are thus of no economic interest. Molybdenite is a semiconductor and can consequently be successfully utilized, along with silicon, in nanoelectronics to artificially separate chemically pure and structurally perfect monomolecular layers of synthetic crystals (Atuchin, 2011).

Electron properties of natural molybdenite broadly vary from sample to sample because of the structural and chemical heterogeneity of its individual crystals. Interaction of admixtures with defects in the crystal structure of the host mineral leads to the accumulation of these admixtures and development of local structured domains with elevated concentrations of these admixtures (Alekseev and Marin, 2012). Enrichment of minerals in certain chemical elements often disturbs the regularity in the atomic structures of these minerals.

Molybdenite $MoS_2$ is characterized by a layered crystal structure. In the planes of the sheets, Mo and S atoms are connected by strong covalent bonds, whereas chemical binding perpendicular to the layers is of the Van der Waals type, very weak and can be easily broken by even a minimal mechanical action. Molybdenite occurs in nature in two polytypes: the overwhelming majority of specimens of this mineral from 200 deposits are its hexagonal 2*H* modification ($a$ = 3.16Å, $c$ = 12.3Å, Z = 2)), the other, strongly subordinate, polytype is 3*R* trigonal rhombohedral ($a$ = 3.16Å, $c$ = 18.33Å, Z = 3) and the rest of the specimens consist of a mix of these polytypes (Khurshudyan *et al.*, 1966; Chukhrov *et al.*, 1968; McCandless *et al.*, 1983; and others). Both polytypes are stable within a broad temperature range. Literature data on the polytypes of molybdenite from high-temperature deposits is still very scarce. For example, molybdenite specimens from the Kamchab pegmatite deposit, S. Africa, contain 44 and 35% of the 3*R* polytype, which bear 700 and 1800 ppm Re, respectively (McCandless *et al.*, 1993). The content of the 3*R* polytype in molybdenite from skarn deposits (Newberry, 1979; McCandless *et al.*, 1993) ranges from 5%

(100 ppm Re) to 30–90% (750 ppm Re). At the same time, this mineral from Pitkjaranta, Karelia and Ak-Kezen', Kazakhstan, consists solely of the 2*H* polytype (Chukhrov *et al.*, 1968).

The principal aim of our research was to elucidate the means of accommodation of admixture atoms in the crystal structure of molybdenite. Among all admixture atoms, Re is the only one always detected in all molybdenite specimens, which contain this element in concentrations from a few ppb to 2000 ppm and even higher (Voudouris *et al.*, 2009). Elevated concentrations of Re, as well as other minor elements, such as W and Fe, are usually found in the rhombohedral 3*R* polytype of the mineral. It has been experimentally demonstrated that crystals of 3*R* molybdenite grow at spiral dislocations, which are produced in the presence of admixtures (Newberry, 1979). At the same time, structural analysis of four Re-rich (0.45–4.2%) molybdenite specimens from northern Greece indicates that the mineral crystallized as its hexagonal 2*H* polytype (Voudouris *et al.*, 2009). Several researchers studying Re accommodation in molybdenite explain this by isomorphism between Re and Mo (Noddack and Noddack, 1935; Pokalov, 1963; Kosyak, 1965; McCandless *et al.*, 1993; and others).

## Methods

In order to elucidate the modes of Re accommodation in the crystal structure of molybdenite, we have examined molybdenite specimens from ten deposits of various genetic types in Mongolia, Magadan area, Transbaikalia and the Urals. The specimens were studied with the use of an electron microscope (BSE images) and X-ray microprobe (Maximyuk and Kulikova, 2013). The morphology of molybdenite in the specimens is very diverse: it occurs as large (0.3–1 cm) aggregates, individual platelets, aggregates of such platelets in quartz and as thin films in fractures (slickensides). Microprobe analysis was carried out using a Camebax-microbeam, in polished sections and epoxy pellets impregnated with molybdenite grains. Aggregates and individual platelets of molybdenite were either perpendicular or parallel to the polished surfaces of the pellets. Sites for their analysis were selected based on BSE images of the molybdenite crystals.

Mo and S concentrations in the mineral were determined using the intensities of the $L\beta_1$ and $K\alpha$ reflections, respectively, at an accelerating voltage of 20 kV and beam current of 25–30 nA, using a PET crystal, with regard for the contribution of the Mo line to the intensity of the $K\alpha$ line of S. Re concentrations were calculated from the intensity of the $L\alpha$ line of Re, using a LiF crystal, with regard for the overlap of the Zn line and with the amplitude discrimination of the signal (the Zn concentration was determined from the $K\beta_1$ line, with regard for the overlap of the W line). For the sake of control, we also made use of the $M\alpha$ line of Re (TAP crystal), which was complicated by the overlaps of lines of W, Pb, Si, Ca and certain other elements that are commonly found in molybdenite.

The standard for Re was high-purity metallic Re and the standards for S, Mo, Zn and W were sulvanite $Cu_3VS_4$, powellite $CaMoO_4$, sphalerite ZnS and scheelite $CaWO_4$. The detection limit of Re in molybdenite was 0.04%. The analytical technique is described in much detail in our earlier publication (Maximyuk and Kulikova, 2013).

Back-scattered electron (BSE) images show the microtopography of the surface of the sample. The images were acquired under a Jeol 6700F with field emission and a cold cathode at an accelerating voltage of 5 kV; crystal morphology was examined in SEI (occasionally LEI and ADD) modes. No chemical composition of mineral was determined in regions where the BSE images were taken.

## Microprobe analysis

Microprobe analysis of the mineral was conducted using its specimens from molybdenum-copper porphyry and quartz-vein greisen deposits. The Re concentrations have been preliminary roughly estimated by colorimetric techniques by G.G. Lebedeva at the Institute of the Mineralogy, Geochemistry and Crystal Chemistry of Rare Elements.

We have not detected any differences in the Re distribution in molybdenite from deposits of various genetic types and the only discernible differences were the concentrations of this element. The X-ray microprobe analysis of molybdenite crystals in planes parallel to its cleavage and perpendicular to it reveal that Re is extremely unevenly distributed in the mineral and that Re concentrations unsystematically vary. Re in concentrations higher than its detection limit (0.04%) but lower than 0.42% were detected at 98 of 284 analyzed spots (i.e., at 35% of the spots) and this proportion practically did not vary at Re concentrations in the specimens varying from

80 to 1100 ppm. The fact that Re may be concentrated within very small domains results in that this element is sometimes not detected when the beam was shifted for a few micrometers away from spots with elevated Re concentrations. Moreover, both Pb and W were determined to behave analogously to Re. An equally uneven Re distribution is also typical of poorly polishable aggregates that typically have a "hillocky" surface topography and bear the highest Re concentrations.

Our microprobe analytical data led us to suggest that the uneven Re distribution in the molybdenite crystals at Re concentrations higher than 0.04% may be explained by defects in the crystal structure of the mineral, namely, by the presence of tiny inclusions of 3*R* molybdenite in a matrix of 2*H* molybdenite. Correlations between Re concentration in molybdenite and the proportion of its 3*R* polytype were mentioned by several researchers. Judging by literature data (Gertsen *et al.*, 2003; Newberry, 1979; McCandless *et al.*, 1993; and others), in spite of the broad scatter of the data, the content of the 3*R* polytype is likely to positively correlate with their Re concentrations. Thereby the contents of the 3*R* polytype generally range from 6 to 36% of the total of both polytypes ($3R + 2H$) at Re concentrations ≤1200 ppm.

## Electron microscopic data

We took BSE images of the molybdenite specimens from the Erdenet, Mongolia and Mys Pavlovich, Magadan area, Mo-Cu porphyry deposits that had been analyzed on a microprobe. The deposits are similar in mineralogy but differ in age and are hosted in different rocks.

Molybdenite is one of the principal ore minerals at the Erdenet deposit and occurs at it in a number of populations. We have studied molybdenite of the main, oldest molybdenite-quartz association. The mineral was found in the form of large (up to a few centimeters across) hexagonal tabular crystals and pockets and contains 760–1035 ppm Re. Molybdenite from the Mys Pavlovicha deposit is coarse-crystalline and is sometimes found as subhedral thick tabular crystals up to 3–5 cm across. According to chemical analyses, the mineral contains 363–393 ppm Re.

Detailed data have been previously obtained on the origin of various morphological features in a great number of various crystals, such as healing cracks (Lemmlein, 1973) and development of dislocations (Landau and Lifshitz, 1987; Novikov, 1975). Modern electron microscopic techniques make it possible to elucidate specifics of crystal growth mechanisms described by these researchers.

Our study of molybdenite at micrometer and submicrometer scales (hundreds of nanometers) indicates that molybdenite crystals can be easily split into sheets. Figure 1 shows SEM images of this splitting in naturally occurring molybdenite. The sheets are usually 0.05–0.10 μm thick and occasionally reach 0.50 μm (Figs. 1a–1f), which corresponds to 40–400 unit-cell parameters and roughly corresponds to the spacing of structural sheets. No sheet splitting have ever been observed even at magnifications as high as ×120 000 (Fig. 1f). The figures clearly show that the thin sheets warp in their margins to form hollow pipes in capillary cracks between split sheets of a crystal. The pipes are sometimes triangular (with rounded angles) in cross section (Figs. 1f, 1h). Molybdenite pipes approximately 0.4 μm in diameter and approximately 4–10 μm long often host minute (some 0.04–0.07 μm across) mineral crystals (Fig. 1b). The pipes are likely filled with solution (because some of the pipes show a meniscus) or a gas phase.

Figure 1d shows that empty space between molybdenite sheets is healed with minute aggregates (no larger than 0.10 μm across), which sometimes penetrate more than one sheet and are perpendicular to their planes. These aggregates resemble dendrites that grew between sheets and oriented them. It is known that material is deposited more rapidly closer to a tapering part of a crack. The material for the growth of the dendrite and healing cracks was mobilized via dissolving the walls of the cracks.

**Molybdenite sample from the Erdenet deposit**. Figure 2 displays SEM images of molybdenite specimens from the Erdenet (Figs. 1a–1d) and Kadzharan (Figs. 1e, 1f) deposits. As seen in Fig. 2a, the surface of the crystal is cut by cracks and displays numerous knobs and pits. In spite of the low magnification of the SEM image (×250) but thanks to the high resolution of the zoomed-in images, it can be seen that the knobs are spiral growth layers of the crystal on steps of the crack (shadows indicate that one side of the crack is somewhat higher than the other) that form spiral dislocations (A–C and E in Figs. 2a–2c). Some of them (B and C in Fig. 2b) show "ledges" with hexagonal sectorial crystals on their tips. Figure 3 (A–C and E, row I) displays geometrical representations of the

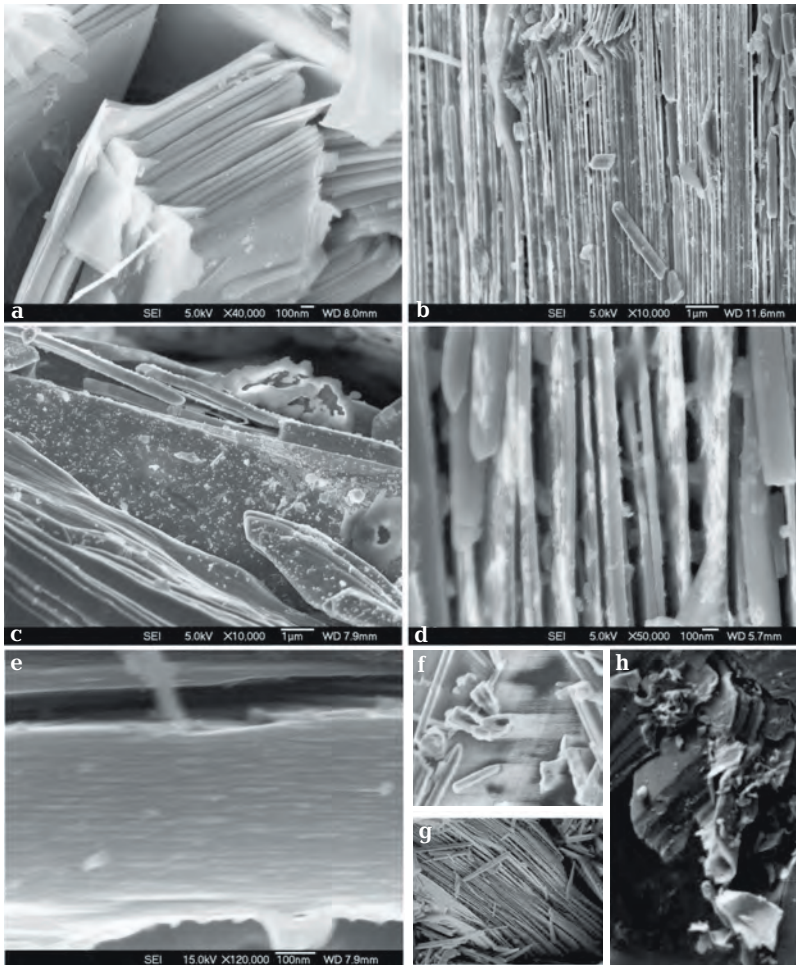


*Fig. 1. Secondary-electron images (SEI) of molybdenite specimens split in thin sheets. (a, c, e) Erdenet deposit, Mongolia, (b, d, f, g), Pavlovich cape, Magadan area and (h) Kharbeiskoe deposit, Polar Urals. Magnification: a – ×40000; b – ×10000; c – ×10000; d – ×50000; e – ×120000; f – ×1000 (fragment); g – ×1000 (fragment); h – ×800 (fragment of an image taken on a Camebax-microbeam).*

morphologies of the defects shown in Fig. 2. The linear dimensions of spiral sheets in Fig. 2 are equal: dislocation A is 4.4 μm (note the pronounced step of the crack), B is 8.4 μm (the hexagon is 3.1 μm), C is 3.9 μm and in E, the outer size of the hexagon is 10 μm. Dislocations B and C are geometrically similar to those in naturally occurring rosettes of molybdenite crystals.

Figure 2a displays a pit 3 μm in diameter (D), which has a hexagonal morphology (Fig. 2b, image fragment zoomed-in by a computer) and the SEM image of another sample from the Erdenet deposit shows a triangular pit (D, Fig. 3 row I). The pits were produced by dissolving molybdenite sheets where dislocations are exposed on the surface.

Defects whose distortion of structural perfectness extends to areas near a certain surface can be microscopically described as discontinuity surfaces. This linear imperfectness that defines the boundary of a displacement (slide) zone in the crystal is referred to as edge dislocation. In Fig. 1g, some sheets do not continue to the right-hand bottom portion. These are extra planes that act as a wedge and perturb the crystal lattice. Above the edge of the extra plane, the sheet spacing is lower than below the edge.

The displacement of an edge dislocation along a normal to the slide plane (climb) is related to mass transfer. The origin and displacement of edge dislocations toward a crystal margin can explain such structural defects as steps at plane margins (circled in the figure) in crystal bends (Figs. 2d–f).

**Molybdenite sample from the Mys Pavlovicha deposit**. Gray shades in the SEI image of molybdenite in Fig. 4 make discernible thin growth layers of the crystal. The growth front envelops various obstacles higher than the layer itself. The concentrations of

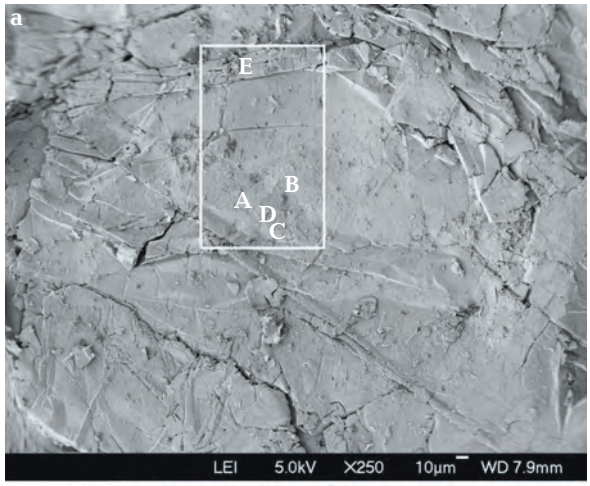


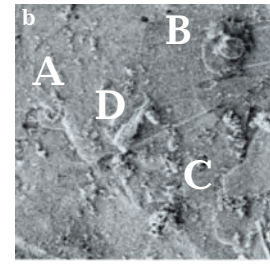


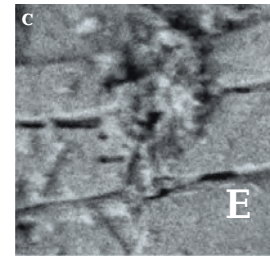



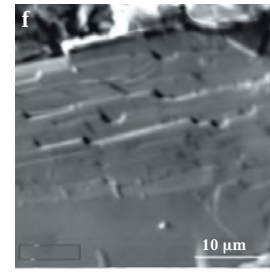


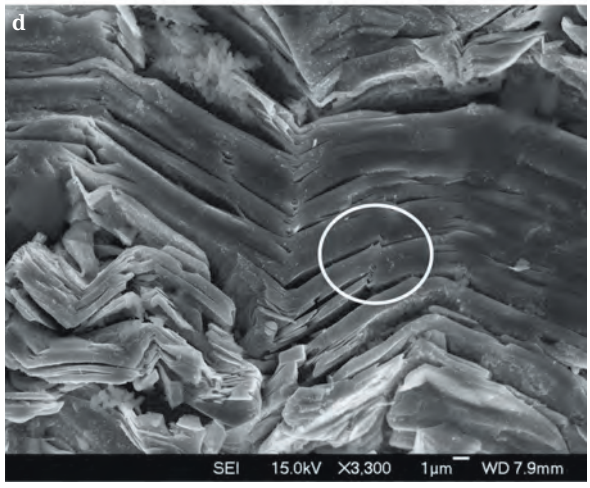


*Fig. 2. SEM images of molybdenite specimens from (a — d) the Erdenet deposit, Mongolia and (e, f) Kadzharan deposit, Armenia. (a) Magnification ×250, letters A, B, C and D denote screw dislocations, D is a negative crystal. The white line contours the region of dislocations. (b, c) This region of dislocations (enlarged image); magnification: d — ×3300; e, f — ×800 and ×2000, respectively (taken on a Camebax-microbeam).*

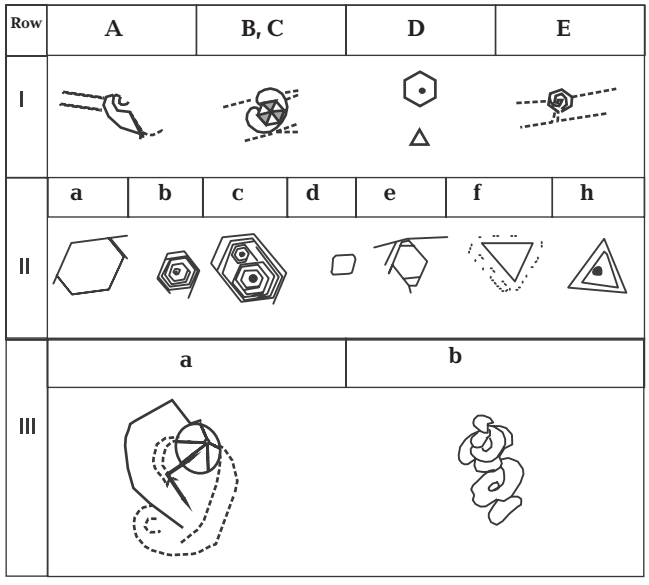


*Fig. 3. Geometry of structural defects in our specimens:*
*row I: screw dislocations (A, B, C and E) and negative crystals (D) shown in Fig. 2a;*
*row II: negative crystals (a-g) shown in Figs. 5a, 5c,5 e, 5g and 5h;*
*row III: a — helical-layered growth contours of a crystal (Fig. 7a), arrows point to a pair of dendrite needles growing from a single center; b —contours of the screw dislocation shown in Fig. 7d.*

Ca and Si admixtures (microprobe data) usually increase along the growth front of a molybdenite sheet, where clusters of minute particles are seen. The following four distinct regions are discernible in the image: (I) a region of relatively smooth surface with pits of certain morphology 2–4 μm across, (II) surface with numerous and diverse pipes up to 30 μm long and <1 μm in diameter, (III) surface with knobs up to 60 μm and (IV) region abounding in structural defects exposed at the surface and precluding the propagation of the growth layer. Smaller domains were selected for detailed studying in each of the regions.

**Region I**. Figure 5 presents a SEI image of this region of the molybdenite sample from the Mys Pavlovicha deposit. The geometry of the pits is shown in Fig. 3 (row II: a–e). The hexagonal pits in Figs. 5a, 5c, 5e are equant negative crystals of the hexagonal 2*H* molybdenite polytype (Figs. 5b, 5d). The geometric shapes of the pits exactly replicate the shape of the crystal itself. The negative crystals are formed via molybdenite redeposition with dissolution and evaporation of the material in a hydrothermal environment. The cavities are shaped, similar to shaping of growing crystals, by a tendency of minimizing the surface energy of the crystals. At intense evaporation and a small enough thicknesses of the surface layers, the holes go all the way through the layers (Fig. 5e), but if the layers are thick (Fig. 5c), layered spiral morphology of the negative crystals is manifested. Evaporation layers should correspond to spiral growth layers, which is explained by spiral dislocations in the crystal, which reach the crystal surface and form steps that are spiral growth centers of the crystal. It is known (Lemmlein, 1973) that layers ranging in thickness from a single unit-cell parameter to a few thousand such parameters often develop on crystals (Fig. 5c). Figures 5a and 5e show dendrites growing from beneath and seen through the holes.

Figures 5g and 5h (see contours in Fig. 3, row II, f and g) display two triangular pits with sides approximately 1 μm. The pits were found in region II. The triangular pits seem to be negative crystals similar to the molybdenite crystal of the rhombohedral 3R polytype (Fig. 5f).

**Region II**. As seen in Fig. 6, this region is characterized by intense growth of dendrites (the cross section of thin needles is ≤0.1 μm). During their early growth, crystals are usually not perfectly shaped and faceted but rather grow in the form of dendrites (Lemmlein, 1973). These are branching individuals that crystallize under unequilibrated conditions, when the edges and apexes of skeletal crystals split following certain laws. The resultant optically disordered subindividuals branch (see, for instance, Fig. 6b). When a little bit differently oriented branches of a single dendrite crystal merge, spiral dislocations develop at their boundary. One of such dislocations

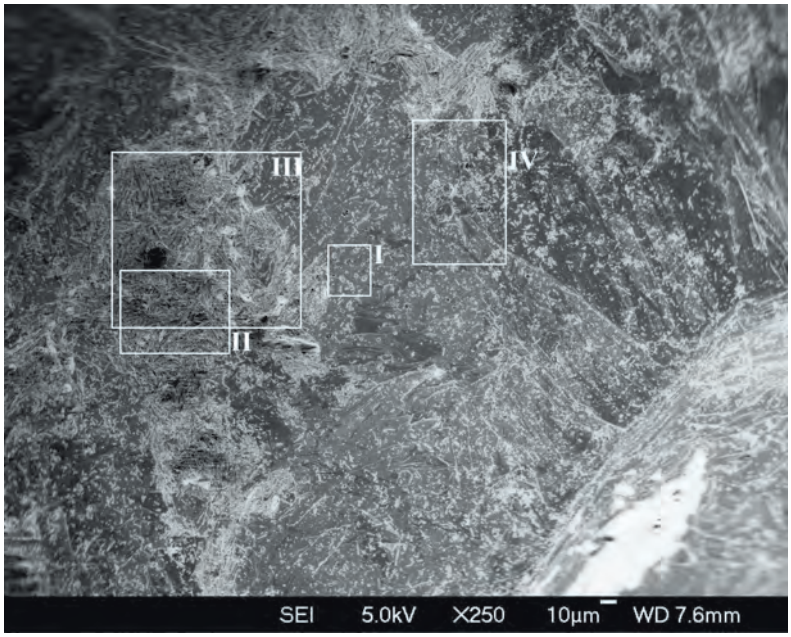


*Fig. 4. SEM image of a molybdenite sample from the Pavlovich cape, Magadan area, magnification ×250. Rectangular contours outline four regions (I, II, III and IV, see text).*

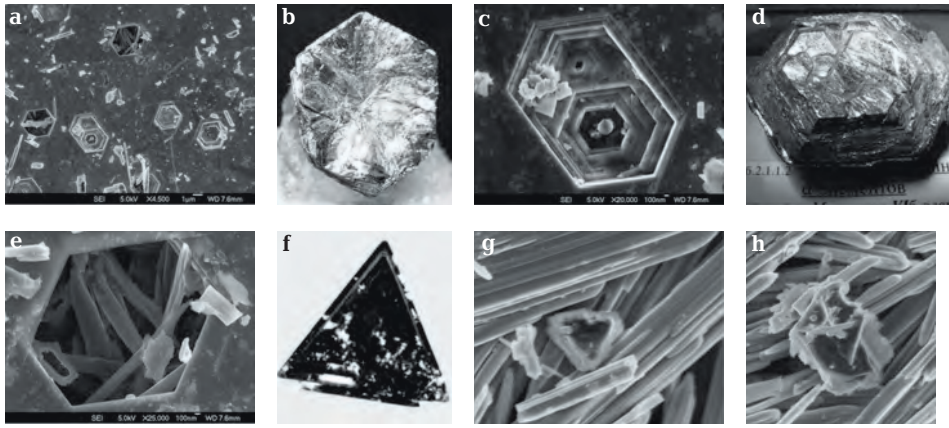


*Fig. 5. SEM images of (a, c, e, g, h) negative molybdenite crystals in regions I and II (Fig. 4) from the Pavlovich cape, (b, d) molybdenite crystals, 2H polytype and (f) molybdenite crystals, 3R polytype.*
*Magnification: a – ×4500, c – ×20000, e – ×25000; g, h – enlarged fragments shown in Fig. 6a. Crystals: Molly Hill, Quebec, Canada (photo: Rob Lewinsky, see http://www.mindat.org/photo-20568.html); d – Selimitsa, Vitosha, Bulgaria (photo: A.A. Evseev, see http://geo.web.ru/druza/m-molib_0.htm); and f – Central Province, Zambia (photo: J. Ralf and I. Chaw, http://www.mindat.org/min-2745.html).*

is displayed in Fig. 7d and the contour of this dislocation is portrayed in Fig. 3 (row III, b).

The richer the system in admixtures, the stronger the branching of the seed crystal and the higher probability that spiral dislocations are generated during further growth of the crystal (Lemmlein, 1973; Novikov, 1975). Compounds prone to crystallize in the form of dendrites commonly generate numerous dislocations (for example, metals).

Region II also shows thin sheets of the crystals rolled into pipes (some of them are exhibited in Figs. 1f, 1h). Several of the pipes are triangular in cross section, likely because of the elastic strain field of the crystal along the lines of edge dislocations. It is known that the imperfectness region of a crystal because of its edge dislocation (it is referred to as the core of dislocations) can be visualized as if enveloped by a cylindrical surface whose axis is the edge of the extra plane (Novikov, 1975; Landau and Livshits, 1987). In contrast to a screw dislocation, the strain field around an edge dislocation does not show a cylindrical symmetry (Novikov, 1975; Landau and Livshits, 1987): it has extension-gliding planes on its one side and compression on the other.

In the presence of admixture atoms, the elastic strain fields of a dislocation and an admixture atom interact and admixture atoms are accumulated at the dislocation. They are attracted to the edge of the extra plane near an edge dislocation and the concentrations of the atoms decrease away from the dislocation (Novikov, 1975). Figure 6d shows a crystal growing within a pipe under the effect of admixture atoms. In the triangular hollows of the pipes, rhombohedral 3*R* molybdenite polytype can grow in the presence of admixtures (Fig. 5f).

Free surfaces, cavities, cracks and dislocations are sources of vacancies in the crystal. The attraction of vacancies accounts for the origin of helical dislocations whose lines form geometrically regular screw (Novikov, 1975). The dislocations thereby acquire an edge component (Fig. 7c). Figure 7f shows the saw-toothed edges of the pipes shaped by geometrically regular spirals.

**Region III.** This region of the crystal (Fig. 4) abounds of dislocations of different types that are closely spaced (their spacing is nevertheless greater than the unit cell parameters). Such dislocations can be considered collectively and integrally (Landau and Lifshits, 1987). The concentration of dislocations commonly growths toward obstacles both in a single glide plane and in parallel planes, at a density reciprocally proportional to the square root of their distance. As the density of dislocations increases, collective effects start to play the main role, i.e., certain properties are now controlled by the interaction of several dislocation groups.

The only interacting force between homonymous edge dislocations (whose extra planes are similarly oriented relative to the gliding plane) in the same gliding plane is repulsion, whereas heteronymous dislocations, conversely, attract one another. The interacting force between parallel edge and screw dislocation is zero. It is much more dif-

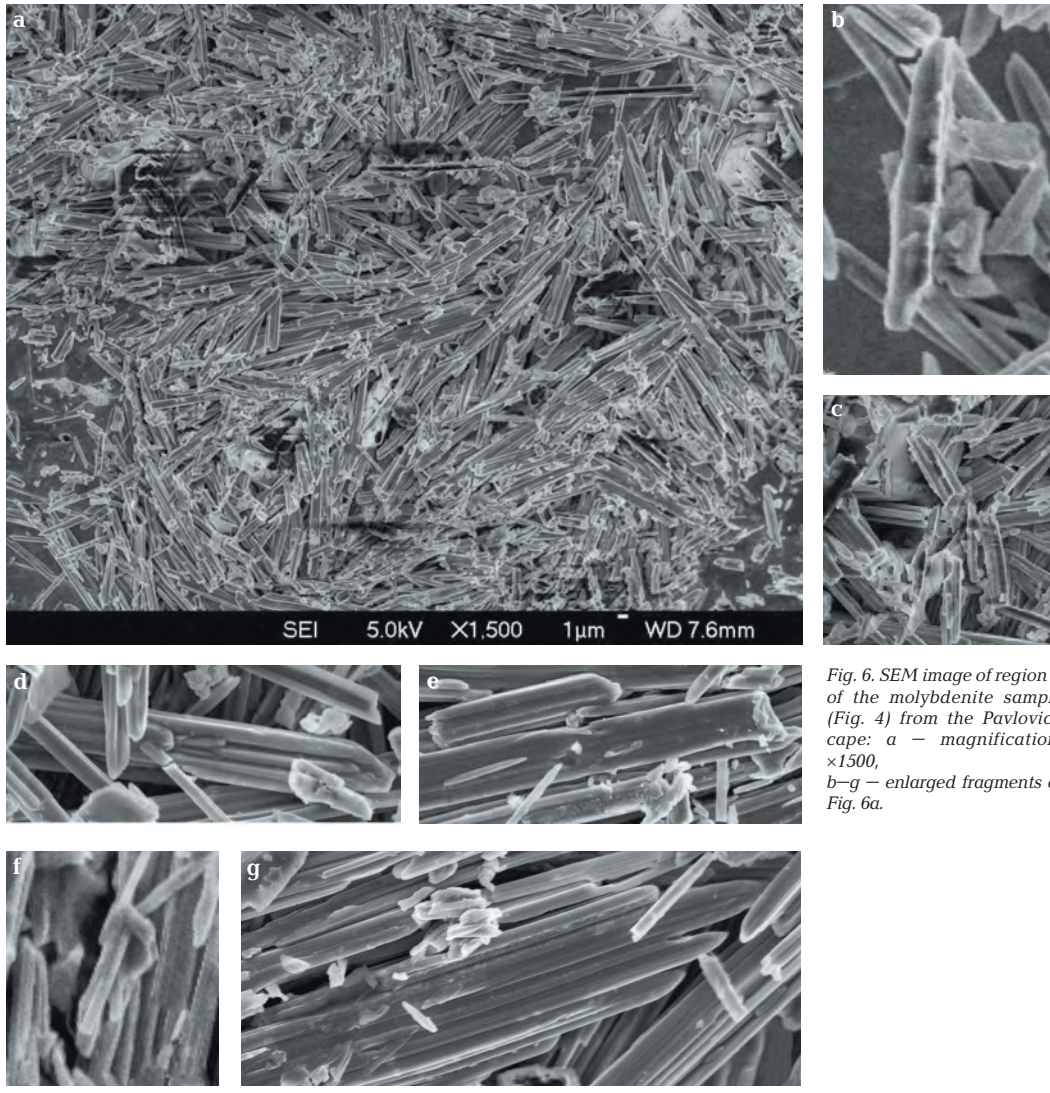


*Fig. 6. SEM image of region II of the molybdenite sample (Fig. 4) from the Pavlovich cape: a — magnification: ×1500, b–g — enlarged fragments of Fig. 6a.*

ficult to evaluate the interacting force between randomly oriented dislocations.

Figure 4 displays the distribution of numerous interacting and propagating mixed dislocations. Figure 7a exhibits a fragment of Region III with discernible crystal growth contours of spiral-layer configuration (Fig. 3, row III, a). The spiral centers of this group of dislocations are spaced 50 μm apart. The spirals growing from these centers are different in their sense. The contours of the spirals are marked by dendrite needles that grow from a single center in perpendicular directions, one of which is tangent to the spiral plane. The growth directions of the needles change to opposite ones likely according to changes in the sense of the tangential and normal strain around the marginal constituent of this group of dislocations (Novikov, 1975). One of the centers of the joint dislocation group is the center of spiral growth of the layers and another center (pit) is the evaporation center of the layer and hence, only the needles of the tangential constituent can be seen in this area.

**Region IV**. This region in Fig. 4 (whose enlarged fragment is displayed in Fig. 7b) concentrates various dislocations: helical, which are perpendicular to the plane, are 0.5 μm across and 2 μm high; edge, which reach the surface at various angles and whose pipes are 2.5 μm in diameter; spiral, which are 2.5 μm in diameter; etc. The arrow within a group of dislocations in Fig. 7b points to a tri-

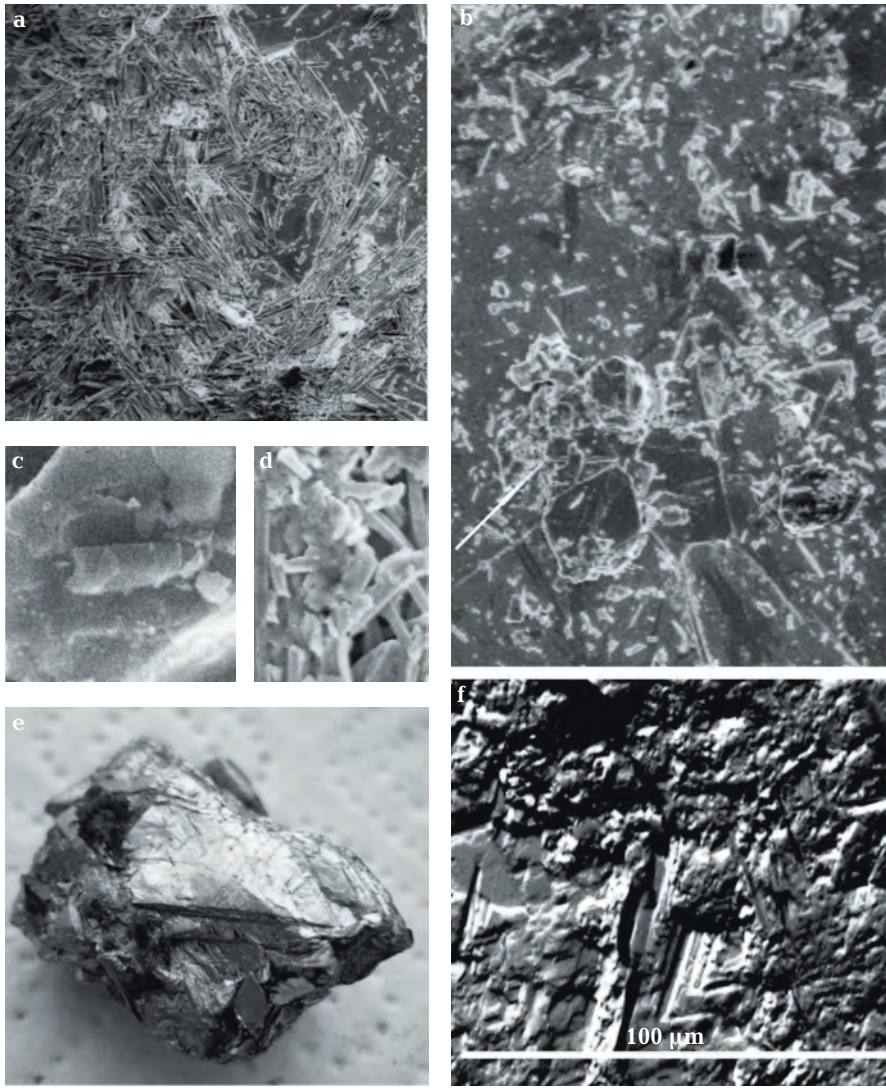


*Fig. 7. Fragments of regions (a) III and (b) IV marked in Fig. 4. Dislocations: (c) helical (Fig. 2d) and (d) screw (Fig. 6a). (f) Fragment of molybdenite image (sample from the Kharbeiskoe deposit, Polar Urals) taken on a Camebax-microbeam (all image fragments are enlarged by a computer). For comparison, the figure shows (e) 3R molybdenite polytype from the Slyudorudnik deposit, Mount Kyshtym, Chelyabinsk area, Urals (see http://форум.хитник.рф/download/file.php?id=2887&mode=view).*

angular tablet (its sides are 7 μm long and its height is 0.2 μm). This minute domain resembles the triangular 3R molybdenite platelets in the sample from the Slyudorudnik deposit in the Chelyabinsk area in the Southern Urals (Fig. 7e). We have earlier obtained analogous results when studying molybdenite from the Kharbeiskoe deposit in the Polar Urals (Fig. 7f).

## Discussion

Thanks to the layered structure of molybdenite, very weak bonds between its structural layers are readily broken under the effect of an even minimal force. Our X-ray microprobe and scanning electron-microscopic data demonstrate that molybdenite crystals can be easily split into thin sheets (0.05 – 0.50 μm thick), which can be readily shifted relative to one another, cracked and form voids. Defects in the crystals can be healed via intense growth of dendrites and the development of screw, edge and other dislocations. The dominant mechanisms generating dislocations in molybdenite crystals is the shift of one crystal part relative to another for a distances ranging one unit-cell parameter to hundreds and even thousands unit-cell distances. The boundary line of this shift can be seen as a line and is a structural imperfectness of the crystal at the nanometer scale. Screw dislocations observable in molybdenite are 1 – 6 μm in diameter.

Admixture atoms are concentrated at dislocations. In a group of dislocations, the greater the density of dislocations, the higher the concentration of an admixture "attracted" to them, with the concentration of the admixture rapidly decreasing away from the core of the dislocations. Surface regions of a sample with an elevated density of screw and other dislocations are usually poorly polishable. X-ray microprobe analysis of our specimens shows than molybdenite with such a characteristic knobby surface bears the highest concentrations of Re and other admixtures, such as W, Pb, Ca, Si and Fe. The accommodation of these elements in molybdenite is likely explained by their occurrence in the form of certain minerals rich in these elements: quartz, powellite, galena, scheelite, Fe oxides, etc. The admixtures are thereby concentrated within very small domains.

The loci of dislocations on the surface of a molybdenite crystal are marked by minute pits, which are negative crystals. The core of dislocations acts as a dissolution and evaporation center. The pits (2–6 μm across) on our specimens have clearly seen faces of negative crystals, which are often hexagonal and similar to hexagonal crystals of the 2*H* polytype of molybdenite. This led us to conclude that this polytype is dominant in our specimens. Triangular pits are negative crystals analogous to crystals of the 3*R* rhombohedral polytype of the mineral, which is very rare.

It has been experimentally demonstrated (Newberry, 1979) that crystals of 3*R* molybdenite grow on screw dislocations that are formed in the presence of admixtures. However, the occurrence of admixtures is only one of the possible reasons for the development of screw dislocations. In the vicinity of an edge dislocations, admixtures are concentrated at the edge of the extra plane. The rolling of the sheets into pipes is likely caused by the elastic strain field of the crystal along the line of edge dislocations. When a crystal grows in a pipe (which are 4–30 μm long, <0.40 μm in outer diameter and are sometimes triangular in cross section) because of admixture atoms, the pipe likely predetermines its structure as the 3*R* polytype.

Microprobe analyses and SEM images of molybdenite specimens make it possible to closely examine minute details in the structure of the mineral and the composition of its small fragments.

Our data indicate that admixture elements are accommodated in molybdenite at its structural defects, first and foremost, dislocations. This pertains not only to Re, an element of undoubted scientific and applied interest, but also to such elements as Si, Ca, Pb, W and Fe.

## Acknowledgments

The authors thank G.N. Trach and N.S. Smirnova for providing us with molybdenite specimens and A.A. Burmistrova for help with conducting the experiments.

## References

*Alekseev V.I., Marin Yu.B.* Structural and chemical heterogeneity of natural crystals and microgeochemical studies in the ontogeny of minerals // Zap. VMO. **2012**. Part CXLI. No. 1. P. 3–21 (in Russian) (translated: Structural and Chemical Heterogeneity of Natural Crystals and Microgeochemical Line of Research in Ontogeny of Minerals // Geol. Ore. Deps. **2012**. Vol. 54. No. 8. P. 589–601.

*Atuchin V.* Interview, Computerra-Online. URL: http://www.computerra.ru/interactive/598591/ (date: March 10, **2011**) (in Russian).

*Chukhrov F.V., Zvyagin B.B., Ermilova L.P., Soboleva S.V., Khitrov V.G.* Molybdenite polytypes and their occurrence in ores // Geol. Ore Deps. **1968**. Vol. 10. No. 2. P. 12–26 (in Russian).

*Gertsen L.E., Petrova N.N., Beketova G.K., Chistilin P.E., Vyatchennikova L.S., Zhukov N.M.* Molybdenite and Re mineralization at Mo-Cu porphyry deposits in the Kuigan-Maibulak ore field, southwestern Balkhash area // Izv. National Acad. Sci. Kazakhstan. Ser. geol. **2003**. No. 2 (382). P. 61–72 (in Russian).

*Khurshudyan E.Kh.* On the genesis of rhombohedral molybdenite polytype // Dokl. Acad. Sci. USSR. **1966**. Vol. 171. No. 1. P. 186–189 (in Russian).

*Kosyak E.A.* X-ray microprobe analysis of a Re-bearing mineral in ores from the Dzhezkazgan deposit // Vestnik Izv. National Acad Sci. Kazakhstan. **1965**. No. 8. P. 52–57 (in Russian).

*Landau L.D., Lifshits E.M.* Theoretical physics. Vol. VII: theory of elasticity, 4th edition. Moscow. Nauka. **1987**. 248 p. (in Russian).

*Lemmlein G.G.* Morphology and genesis of crystals. Moscow. Nauka. **1973**. 328 p. (in Russian).

*Maximyuk I.E., Kulikova I.M.* Modes of Re accommodation in molybdenite from deposits

of various genetic types // Zap. RMO. **2013**. Part 142. No. 2. P. 94—106 (in Russian).

*McCandless T.E., Ruiz J., Campbell A.R.* Rhenium behavior in molybdenite in hypogene and near-surface environments: implications for Re-Os geochemistry // Geoc. et Cosmoc. Acta. **1993**. Vol. 57. № 4. P. 889—905.

*Newberry R.J.J.* Polytypism in molybdenite (II): relationships between polytypism, ore deposition/alteration stages and rhenium contents // Amer. Mineral. **1979**. Vol. 64. № 7—8. P. 768—777.

*Novikov I.I.* Defects in the crystal structure of metals. Moscow. Metallurgiya. **1975**. 208 p. (in Russian).

*Noddack I., Noddack V.* Geochemistry of Rhenium // Major ideas in geochemistry. Leningrad. **1935**. Issue 2. P. 73—110 (in Russian).

*Pokalov V.T.* On the mode of Re accommodation in molybdenite // Mineral resources. Moscow. VIMS. **1963**. Issue 7. P. 179—181 (in Russian).

*Voudouris P.C., Melfos V., Spry P.G., Bindi L., Kartal T., Arikas K., Moritz R., Ortelli M.* Rhenium-rich molybdenite and rheniite in Pagoni Rachi Mo-Cu-Te-Ag-Au prospect, Northern Greece: implications for the Re geochemistry of porphyry-style Cu-Mo and Mo mineralization // Canad. Mineral. **2009**. Vol. 47. No 5. P. 1013—1036.